

## **PERSPECTIVE**

View Article Online
View Journal | View Issue



**Cite this:** *New J. Chem.*, 2020, **44**, 3546

Received 21st December 2019, Accepted 31st January 2020

DOI: 10.1039/c9nj06330g

rsc.li/njc

# Recent advances in organic dyes and fluorophores comprising a 1,2,3-triazole moiety

Damien Brunel 🕩 \* and Frédéric Dumur 🕩 \*

Since the discovery of the copper catalyzed azide alkyne cycloaddition in the early 2000s, tremendous efforts have been devoted to enlarging the scope of applications of this relatively simple to handle reaction. The chemistry of dyes has not been excluded from this enthusiasm so that a wide range of compounds have been synthesized over the years. Several key elements have sustained such research activity, such as the possibility to fine tune the photophysical properties, the easiness of structure screening in order to optimize the optical properties or the thermal stability of the triazole moiety. In this review, an overview of different dyes as well as their applications is reported.

#### 1 Introduction

The independent discovery at the beginning of the 21st century of the copper-catalyzed version of the well-known azide-alkyne 1,3-dipolar cycloaddition by Medal and then Sharpless has enabled the introduction of the concept of click chemistry in modern chemistry.<sup>1,2</sup> This cycloaddition reaction, also known as the Huisgen reaction and reported for the first time by Huisgen in the 60s,<sup>3</sup> has revolutionized the way to create molecules by its simplicity and its efficacy. Indeed, click chemistry consists in mimicking Nature, which fabricates natural substances by joining together elemental building blocks by means of a simple and easy reaction. More generally, click chemistry is based on reactions where two specific functional groups react together in soft conditions i.e. in non-dangerous solvents and at room temperature, without formation of by-products and in high yields. Moreover, the structures of the potential substrates being limitless, an infinite diversity of structures can be formed. Benefiting from this versatility, click chemistry was notably used to produce numerous molecules with applications ranging from pharmaceuticals<sup>4-6</sup> to materials,<sup>7,8</sup> modified alkaloids,9 carbohydrate chemistry,10 crop protection products (antifungal or pesticides), 11,12 etc. 13,14 The azide alkyne cycloaddition involves a reaction between an azide and an alkyne, producing a stable 1,2,3-triazole ring. The thermal cycloaddition of an azide and an alkyne furnishes most of the time a mixture of two regioisomers: the 1,4-disubstituted triazoles and the 1,5-disubstituted triazoles. Selectivity between the two regioisomers can however be obtained by a careful selection of the metal catalyst. Thus, CuAAC (copper catalyzed azide alkyne cycloaddition) is a convenient way to produce specifically the 1,4-triazole ring whereas ruthenium-catalyzed azide-alkyne cycloaddition (RuAAC) only provides the 1,5-regioisomers (see Scheme 1).

If click chemistry has been extensively studied for the design of molecules with biological applications, use of click chemistry for the design of chromophores and photoluminescent molecules is more scarce, even if the triazole ring can be advantageously used to connect under mild conditions an electron-donating group to an electron accepting group. 15 Notably, the triazole ring offers a unique opportunity to give elaborate push-pull dyes which are now commonly used as photoinitiators of polymerization. 16-23 Consequently, this heterocyclic five-membered ring is mainly used as a  $\pi$ -conjugated spacer ensuring electronic communication between the electron-donating and accepting moieties. In this review, an overview of the different chromophores and photoluminescent push-pull molecules prepared by click chemistry is presented. Beyond the synthesis of these compounds, the different applications in which these different structures have been used are also presented.

$$R_1-N_3$$
 +  $=$   $R_2$   $\xrightarrow{\Delta}$   $R_1-N_2$  +  $R_1-N_2$  +  $R_1-N_2$  +  $R_1-N_3$  +  $R_2$  +  $R_1-N_3$  +  $R_2$   $R_1-N_3$  +  $R_1-N_3$  +  $R_1-N_3$  +  $R_2$ 

**Scheme 1** The different types of cycloadditions based on the combination of an alkyne and an azide.

Aix Marseille Univ, CNRS, ICR, UMR 7273, 13397 Marseille, France

## 2. Push-pull molecules and light responsive organic molecules containing triazoles

The association of an electron donor and an electron acceptor connected by means of a triazole ring was done for the first time in 2005 by Blanchard-Desce and coworkers. 24,25 To examine the specificity introduced by the presence of the triazole ring in the push-pull dyes, a comparison was established between a series of dyes previously reported in the literature by the same authors and comprising alkene or alkyne spacers (i.e. compounds 1-3) and the newly developed triazole-based dyes 4 and 5 (see Fig. 1).26

Starting from the commercially available tris(4-ethynylphenyl)amine 6, 4,4'-diethynylbiphenyl 7 and N-(4-azidophenyl)-Nhexanoyl-hexanamide 8, the two products 4 and 5 could be formed in good yields, 68 and 86% respectively (see Scheme 2). The optical properties of the two dyes 4 and 5 were compared with those of their analogues 1-3 comprising  $\pi$ -conjugated spacers classically used for the design of push-pull dyes (see Table 1).27 While comparing the absorption properties of the star-shaped dyes 1 and 4, a hypsochromic shift of ca. 40 nm of the position of the intramolecular charge transfer (ICT) band could be observed for 4 compared to that of 1. Similarly, a twofold reduction of the photoluminescence quantum yield (PLQY) for 4 compared to that of 1 was also detected. A more severe reduction of the PLQY was demonstrated for 5, the latter being divided by a factor 3.9 compared to that of its analogue 2. While examining the order of the ICT bands, the most blue-shifted ICT band was found for 5 bearing the triazole ring, followed by

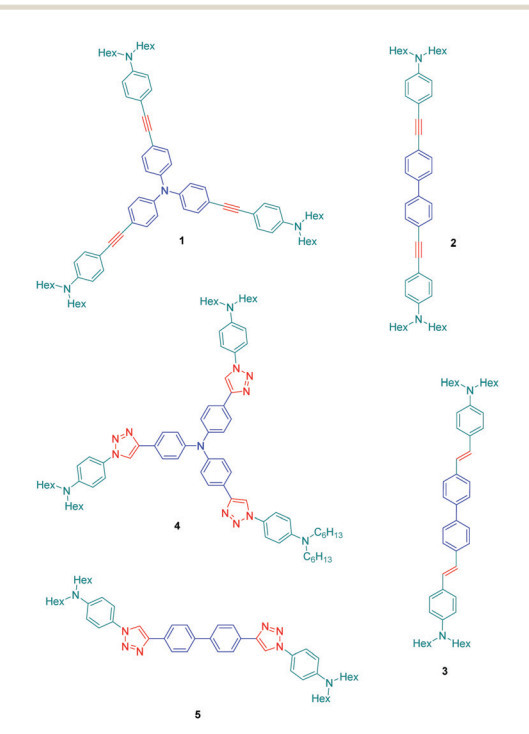


Fig. 1 Structures of triazole-based dyes 4 and 5 and their alkyne/alkene bridged analogues 1-3.

Scheme 2 Synthetic pathways to 4 and 5

Table 1 Photophysical characteristics of triazole-based dyes 1-5 in toluene

Molecules	$\lambda_{\rm abs}{}^a({\rm nm})$	$\lambda_{\mathrm{em}}^{a} (\mathrm{nm})$	$\Phi_{ m F}^{\;\;b}$	Stokes shift (cm <sup>-1</sup> )	Ref.
1	385	411	0.77	1634	6
4	347	387	0.49	3000	9
2	374	424	0.90	3200	9
3	401	456	0.84	3000	9
5	325	391	0.23	5100	6

<sup>&</sup>lt;sup>a</sup> Recorded in toluene. <sup>b</sup> Photoluminescence quantum yield.

2 and 3 bearing an alkene and an alkyne spacer respectively. Therefore, it can be concluded that the 1,2,3-triazole ring is the worse candidate to connect the electron donor to the electron acceptor, the blue-shift of the ICT band being indicative of a lack of electronic communication between the two partners.

If the detrimental effect of the 1,2,3-triazole ring on the electronic delocalization of 4 and 5 could be easily evidenced with a significant reduction of the PLQYs and a blue-shift of the ICT bands compared to those of 1-3, conversely, the greatest Stokes shifts were determined for these dyes. Indeed, if Stokes shifts of 3200 and 3000 cm<sup>-1</sup> were found for 2 and 3 respectively, this value increased up to 5100 cm<sup>-1</sup> for the triazole-based dye 5. Therefore, based on the large Stokes shifts, it can be concluded that a major electronic redistribution occurs prior to emission. Following this pioneering work, several derivatives still based on the triphenylamine electron donor were prepared and examined for their photophysical properties. In fact, triphenylamine is at the basis of numerous compounds developed for photovoltaic applications due to its remarkable charge transport ability and its low oxidation potential. 28-36 The chemical structures of the different triphenylamine-based dyes 9-11 synthesized by click chemistry are presented in Fig. 2.37 To prepare 9-11, mono, bis and tris-ethynylsubstituted triphenylamines 12-14 were engaged in reactions with 3-(4-azido-2,5-bis(hexyloxy)phenyl)-2-cyano-acrylic acid 15

HOOC CN CeH13 COH NC COH NC COOH NC CO

Fig. 2 The three triphenylamine-based dyes **9–11** and the reference dye **N719** 

in a THF-H<sub>2</sub>O mixture using sodium ascorbate and copper sulfate as the catalysts. **9-11** could be prepared with reaction yields ranging from 77 to 87%. 3-(4-Azido-2,5-bis(hexyloxy)phenyl)-2-cyanoacrylic acid **15**, which constitutes the precursor of the electron accepting part of the push-pull dyes **9-11**, is substituted with a cyanoacetic acid moiety favourable for the adsorption of the dye onto the TiO<sub>2</sub> electrode. This intermediate could be prepared in a 4-step procedure depicted in Scheme 3.<sup>33,38</sup>

OCeH13

Propane-1,3-diol, BF3 OEt2
toluene, 8 h, reflux, 87%

OCeH13

16

17

Na, 78°C,
THF

THF

2) Na, 20, 20, 41, 20
3) HCl/H<sub>2</sub>O OHC

OCeH13

Frequence acid (1 équiv), pipendine

MeCN, 12 h, reflux, 89%

HOOC

NaHCO3, ascorbic acid,
CuSO4, 84, 0

THF/H<sub>2</sub>O; 2/1

85% yield

NaHCO3, ascorbic acid,
CuSO4, 84, 0

THF/H<sub>2</sub>O; 2/1

NAHCO3, ascorbic acid,
CuSO4, 84, 0

NAHCO

Scheme 3 Synthetic routes to 3-(4-azido-2,5-bis(hexyloxy)phenyl)-2-cyanoacrylic acid **15** later used for the synthesis of **9-11**.

Notably, after protection of the aldehyde group of **16** with propane-1,3-diol, acetal **17** could be formed in 87% yield. Finally, the azido group could be introduced in 87% yield using *n*-butyl lithium as the base. After deprotection of the aldehyde, a Knoevenagel reaction carried out on **18** with cyanoacetic acid provided the targeted intermediate **15** in 89% yield.

9-11 were analysed by UV-visible absorption spectroscopy and cyclic voltammetry, and finally characterized as potential candidates for dye sensitized solar cells (DSSCs). The efficiencies of the corresponding solar cells remained moderate, the photon-to-electron conversion efficiency peaking at 3.00% for 9 (see Table 2). Interestingly, a reduction of the energy conversion efficiency was found while increasing the number of branches on the triphenylamine moiety, which was attributed to a reduced density of molecules on the TiO2 anode. Indeed, by increasing the number of branches, a dramatic increase of the molecule size occurs requiring more space to be attached on the electrode, thus lowering the photon-to-electron conversion. All dyes showed a broad absorption band in the solid state ranging between 300 nm and 500 nm with a long tail extending until 700 nm. More precisely, for 9 and 10, the absorption spectra showed two peaks, one around 310 nm attributable to  $\pi$ - $\pi$ \* transitions and a second one at 400 nm corresponding to the ICT band. Conversely, for 11, a strong overlap of the  $\pi$ - $\pi$ \* transitions and the ICT band was found so that the absorption band at high energy was detected as a simple shoulder of the ICT band. The bathochromic shift of the ICT bands from 11 to 9 can be explained by a higher polarity of the molecule upon reduction of the branch number, facilitating the delocalization of electrons upon photoexcitation.

Theoretical calculations revealed the HOMO and LUMO energy levels of 9-11 to be spatially well-separated thanks to the presence of the triazole group. Indeed, the HOMO level was determined as being centered on the triphenylamine moiety whereas the LUMO level was localized on the anchoring group (i.e. the cyanoacetic acid group). Due to this well-defined separation between the HOMO and LUMO energy levels, efficient injection of the electrons into the conduction band of  $\text{TiO}_2$  is expected upon photoexcitation. Cyclic voltammetry showed the dyes to be good candidates for photovoltaic applications due to their energy levels perfectly fitting with those of the adjacent layers. Notably, the position of the LUMO level at -3.50 eV is favourable for electron injection into the conduction band of  $\text{TiO}_2$ .

Table 2 Properties of the triphenylamine-based dyes 9-11

Dye	$\lambda_{\max}^{a}$ (nm)	$\epsilon^b (10^4 \text{ M}^{-1} \text{ cm}^{-1})$	$E_{\rm red}$ (V)/ LUMO <sup>c</sup> (eV)	$E_{\text{ox}}$ (V)/ HOMO <sup>d</sup> (eV)	η (%)
9	312, 388	3.28, 1.51	-0.86/-3.50	0.96/-5.32	3.00
10	320, 405	6.00, 3.73	-0.83/-3.54	0.91/-5.28	2.13
11	348	6.08	-0.81/-3.51	0.98/-5.3	1.58
N719	_	_	_	_	4.86

 $<sup>^</sup>a$  In dioxane with  $C = 1 \times 10^{-5}$  M.  $^b$  Molar extinction coefficient at  $\lambda_{\rm max}$  in solution.  $^c$  Estimated from the onset reduction potential/calculated with the formula  $E_{\rm LUMO}$  (eV) =  $-(E_{\rm red} + [4.8 - E_{\rm (Fe/Fe^+)}])$  eV.  $^d$  Estimated from the onset oxidation potential/calculated with the formula  $E_{\rm HOMO}$  (eV) =  $-(E_{\rm ox} + [4.8 - E_{\rm (Fe/Fe^+)}])$ .

Perspective

Similarly, the position of the HOMO level at -5.30 eV is lower than that of the I<sup>-</sup>/I<sub>3</sub><sup>-</sup> redox potential so that the different dyes can be efficiently regenerated during device operation. <sup>39,40</sup> Parallel to the molecular size, which increases with the number of branches on the triphenylamine core, the low energy conversion efficiency could also be assigned to the limited absorption ability of triazole-linked push-pull dyes 9-11, only partially covering the solar spectrum. On the contrary, the reference device fabricated with N719 could provide a higher conversion efficiency by overcoming this drawback (see Table 2). Notably, N719 exhibits two main absorption bands at 380 and 550 nm so that its absorption spectrum almost extends from 350 until 800 nm.

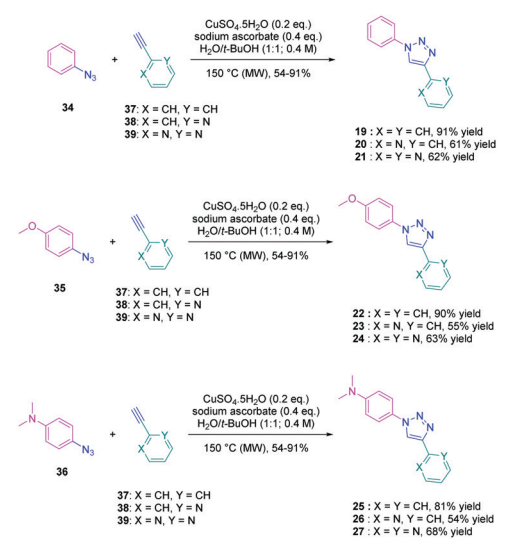
To establish a clear structure-performance relationship, the synthesis of numerous derivatives is a prerequisite. This hard work was notably done with a series of twelve dyes (19-30) prepared by click chemistry and comprising a 1,2,3-triazole ring. In this context, guidelines concerning the introduction of 1,2,3-triazole rings in push-pull dyes could be established. The photophysical properties of these dyes were compared to an analogue series (31-33) composed of 3 dyes bearing a phenyl spacer instead of the triazole ring.<sup>41</sup> In fact, to clearly evidence the real impact of the triazole ring on the photophysical properties, two series of triazole-based dyes were prepared, the first one (19-27) bearing the five-membered ring in an inverted position compared to the second one (28-30), generating two groups of regioisomers (see Scheme 4 and Fig. 3).

From a synthetic point of view, the first series (19-27) was prepared while using the azide group attached to the electrondonating moiety (34-36). The click reaction carried out under microwave irradiation could provide the different dyes with reaction yields ranging from 54 to 91% upon irradiating the solutions for 30-60 minutes. On the contrary, for the inverted series, the synthetic procedure should be modified for the preparation of 29 and 30, 2-azidopyridine and 2-azidopyrimidine being less reactive than azidobenzene due to the formation of the tetrazole ring by tautomeric equilibrium. In this context,

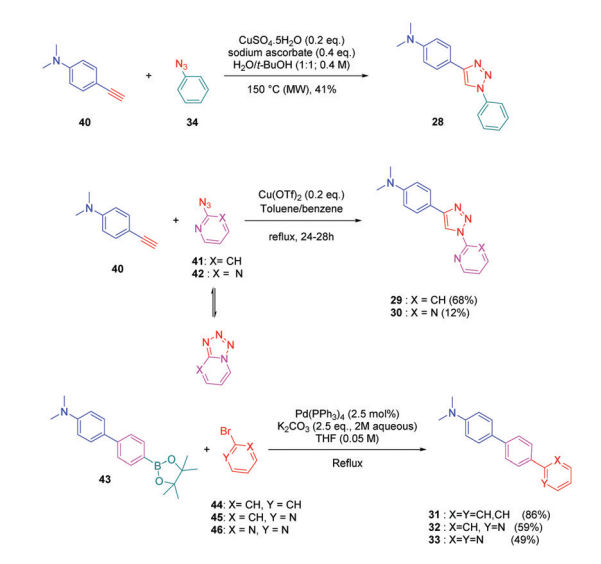
Fig. 3 Second series of push-pull molecules 28-33

classical thermal conditions were used. By refluxing in toluene with traces of benzene and while using copper triflate as the catalyst, 29 and 30 could be prepared in 68% and 12% yield respectively (see Scheme 5). Noticeably, if traces of benzene in toluene seem to be required for the reaction to proceed, no justification for its presence was mentioned by the authors. Finally, the three reference compounds 31-33 were obtained by a Suzuki cross-coupling reaction of bromobenzene, bromopyridine, or bromopyrimidine with the corresponding boronic ester (see Scheme 5). 31, 32 and 33 could be obtained with reaction yields ranging from 49 to 86%.

The photophysical properties of the three series (19-27, 28-30, and 31-33) were examined to explore the exact role of the triazole spacer in the intramolecular charge transfer process. It has to be noticed that prior to this work, a similar comparison was made from a theoretical point of view by Catan and coworkers of 25 and 28 and the conclusions are consistent with those found in this work. 42,43 A summary of the absorption properties is provided in Table 3. As first findings, the different dyes 19-27 showed no or only weak emission in dichloromethane. Precisely, no emission could be detected for all dyes comprising a benzene ring as the electron donor. While comparing the variation of the absorption maximum for the same electron acceptor, a red-shift of the absorption maximum with the electron-releasing ability of the



Scheme 4 Chemical structures and synthetic routes to 19-27.



Scheme 5 Synthetic routes to 29-33

**Table 3** UV-visible characteristics of push-pull molecules reported in ref. 27

Dyes	$\lambda_{ m abs}^{\ \ a}  ( m nm)$	$\varepsilon^a (\mathrm{M}^{-1} \mathrm{~cm}^{-1})$	λ <sub>em</sub> <sup>a</sup> (nm)	$k^b$ (cm <sup>-1</sup> )
19	250, 266 (sh), 272 (sh), 282 (sh), 289 (sh)	23 140	n.o. <sup>c</sup>	_
20	286	23 140	n.o. <sup>c</sup>	_
21	255	4020	n.o. <sup>c</sup>	
22	256, 267 (sh), 273 (sh)	25 120	n.o. <sup>c</sup>	
23	282 (sh), 289 (sh)	25 600	n.o. <sup>c</sup>	_
24	287	27 180	392	6087
25	263	24 380	n.o. <sup>c</sup>	_
26	286 (sh), 302	20 940	396	12729
27	306	23 920	413	22048
28	309	20 020	454	27 609
29	270 (sh), 302	28 480	438	23228
30	271 (sh), 296, 305 (sh), 345 (sh)	27 660	470	26593
31	268 (sh), 287, 310 (sh), 345 (sh)	16 760	n.o. <sup>c</sup>	_
32	325	34 320	419	13028
33	337	27 640	449	18636

<sup>&</sup>lt;sup>a</sup> Determined in dichloromethane with  $C=5~\mu\mathrm{M}$ . <sup>b</sup> Slope of the linear correlation of the Stokes shift with the solvent orientation polarizability determined from the Lippert–Mataga plots. <sup>c</sup> Not observed.

donor was observed. Parallel to this, by improving the electronwithdrawing ability of the acceptor, a red-shift of the absorption maximum was similarly observed. While comparing with the reference series 31-33 comprising a benzene ring as the spacer, a larger red-shift of the absorption maximum with the donor strength was found ( $\Delta \lambda_{\text{max}} = 26 \text{ nm}$ ) for this series (31–33) compared to the series (19-27) comprising the triazole group  $(\Delta \lambda_{\text{max}} = 7 \text{ nm})$ . This higher shift of the absorption maximum was assigned to a higher charge redistribution upon photoexcitation, evidencing better conjugation between the donor and the acceptor when a benzene ring is used as a spacer. The higher conjugation degree for the benzene-based series was also demonstrated while comparing the absorption maxima for 28 and 31, respectively detected at 302 and 323 nm. Finally, the solvatochromism of the different dyes was rationalized using the Lippert-Mataga equation. 43 In all cases, a linear correlation was found, demonstrating the validity of the model. In this equation, the variation of the Stokes shift with the solvent polarity is examined, and the slope of the plots is directly related to the difference existing between the dipole moments in the ground and the excited state. Logically, for identical electron donors, a steeper slope was found while increasing the electron-accepting ability. But a deeper insight into the linear correlations unveiled more complex processes. Notably, comparison of the slopes for 28 and 31 revealed similar values, demonstrating that a similar charge redistribution occurs upon excitation. However, examination of the absorption and emission maxima of 28 and 31 also evidences the two maxima to be red-shifted for 31 compared to 28, consistent with a higher conjugation degree for the dyes comprising a benzene spacer. Therefore, it was concluded from these different results that if better electronic conjugation exists in the ground state for the dyes (31-33) comprising a benzene spacer, higher charge transfer occurs for the triazole-based dyes (19-27) comprising a strong electron acceptor such as a pyridine or a pyrimidine moiety. Conversely, similar charge transfer is observed for the dyes comprising a weak electron acceptor such as benzene.

Comparison of the regular series (25, 26 and 27) with the inverted series (*i.e.* 28, 29, and 30) revealed redshifted absorption for the inverted series. Comparison of the slopes of the Lippert-Mataga correlation of the regular and inverted series for dyes (25–27 vs. 28–30) comprising a strong electron acceptor also revealed the slopes for the inverted series (28–30) to be more pronounced than those of the regular series (25–27).

From these observations, it was concluded that for the inverted series, the triazole ring was acting as an electron acceptor. Overall, the orientation of the triazole ring in the regioisomers can efficiently influence the photophysical properties of the push–pull dyes. For most of the abovementioned dyes, crystals could be grown so that their Non-Linear Optical (NLO) response could be examined. However, as a prerequisite, only structures crystallizing in a non-centrosymmetric arrangement could be considered for their capabilities to produce a non-linear response. Among all dyes, only 22, 23 and 24 were analyzed for their Second Harmonic Generation (SHG) efficiencies while using potassium dihydrogen phosphate (KDP) as a reference.

As predicted by the two-state model,<sup>44</sup> the best non-linear response was obtained for the dye exhibiting the strongest charge redistribution upon excitation and the non-linear response of 24 was 80 times higher than that of KDP. Conversely, the SHG efficiencies of 22 and 23 were 3.4 and 6 times higher than that of KDP. Prior to this work, numerous studies were carried out by the group of Fröhlich et al. on push-pull dyes comprising the 1,2,3-triazole ring as an electron-acceptor. In this field, the first report was published in 2011 with 47 crystallizing in the space group  $P2_12_12_1$ . This compound could be prepared in two steps, by thiophene-ring fragmentation (TRF) of (3-bromo-5-methylthiophen-2-yl)trimethylsilane. 45-47 Following the formation of the intermediate enyne, the click reaction of azidobenzene with the enyne derivative could provide the expected dye as the unique 1,4-regioisomer in 75% yield by using microwave irradiation (see Scheme 6).

Conversely, all attempts of synthesis using thermal conditions could only furnish 47 in 58% yield after 18 hours of heating at 50 °C. Importantly, the *Z*-geometry of 47 was of crucial importance to produce none-centrosymmetric crystals. Examination of the SHG response while exciting at 1064 nm revealed the NLO response to be two times higher than that of KDP.

Considering that the 1,2,3-triazole group acts as an electron acceptor in these structures, 47 was revisited in a more extended study (47 and 51–59) in which ten different groups were attached onto the five-membered ring (see Fig. 4).<sup>48</sup>



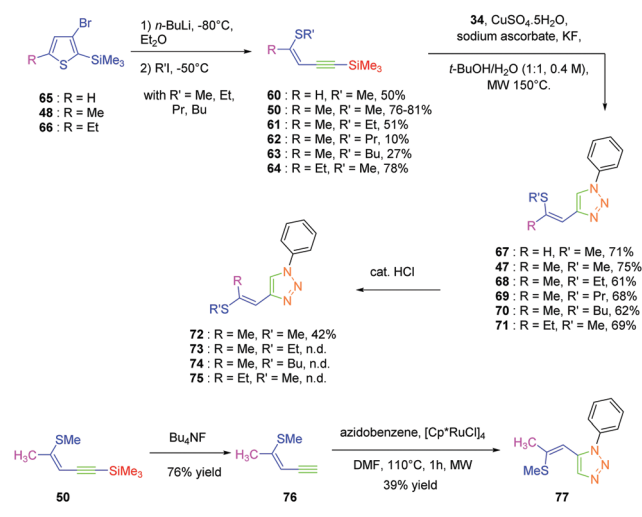
Scheme 6 Synthetic route to the push-pull dye 47.

Fig. 4 Chemical structures of 47 and 51-59

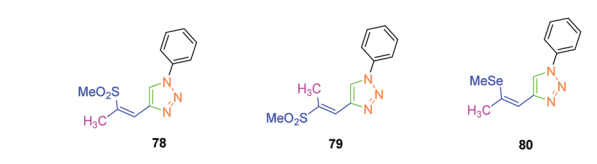
While examining the substituent effects, substitution of the 1,2,3-triazole ring with aromatic rings (54-56) was determined as being preferable over vinylic (57-59) or aliphatic groups (51–53). Finally, for aromatic rings, the methylsulfone group (55) proved to be the best substituent for maximizing the hyperpolarizability tensors. Compared to 47 comprising an unsubstituted aromatic ring, an enhancement of the NLO response by a factor 3.5 was obtained for 56 substituted with a sulfone moiety (see Table 4).

Click chemistry being a versatile technique enabling one to perfectly control the regioselectivity, a comparison between 1,2 and 1,4-regioisomers was established. 49 Different groups were introduced onto the electron-donating thiol moiety, namely, methyl, ethyl, propyl and butyl groups. The different alkynes 50 and 60-64 were obtained by ring-opening of the thiophene derivatives 48, 65, and 66. By applying a copper-catalysed click reaction to 50 and 60-64, six different dyes 47 and 67-71 could be prepared with reaction yields ranging from 61 to 75%. Reflux in the presence of a catalytic amount of acid (HCl) could partially isomerize the Z-isomers 47, 68, 70 and 71 into the E-isomers 72, 73, 74 and 75 respectively in moderate yields (see Scheme 7). Indeed, for all dyes 47 and 67-75, preparative thin layer chromatography (TLC) was required to separate the two isomers, providing in turn the E-isomers only in low yields. On the contrary, the ruthenium-catalyzed click reaction selectively furnished the 1,2-regioisomer. In this last case, only one derivative was prepared, namely 77 in 39% yield, starting from 76 formed by deprotection of the silvl group of 50. Examination of the crystal structures of the different dyes revealed 70, 71, 72 and 77 to be unsuitable for NLO measurements due to centrosymmetric crystallization. Finally, the SHG signal detected for the 4-series was relatively low for two dyes i.e. 47 and 68 and no signals were detected for the others.

Isomerization of the double bond only provided the 72-74-series crystallizing in a centrosymmetric arrangement. Modification of the substitution on the 1,2,3-triazole ring did not significantly modify the NLO response of 77, approaching that of its 1,4-regioisomer 47. Upon oxidation of the sulphur atom (78 and 79), the opposite situation to that found for the previous series could be created. Oxidation of sulphur to sulfone converted the electron-donating



Scheme 7 Synthetic route to 47, 67-71 and 77



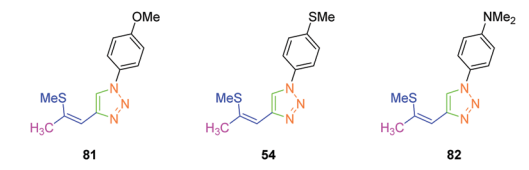
Chemical structures of 78-80

group (sulphur) to the electron-accepting group (sulfone), inverting the push-pull effect. Two stereoisomers were prepared, namely 78 and 79 differing in the configuration of the double bond. While comparing 74 with its parent 47, an enhancement of the NLO response by about 45% was found. Finally, the best results were obtained with the selenium-based analogue of 47 i.e. 80 (see Fig. 5). In this last case, the NLO response was enhanced by a factor of 20, resulting from the increased electron density in the  $\pi$ -conjugated system.

In 2017, the highest SHG efficiency ever reported for this family of dyes was reported by the same authors.<sup>50</sup> Interestingly, a great deal of effort was devoted to improving the synthetic route to these dyes with regards to the safety, the selectivity and the quantity of materials available at each step. By substituting 81, 54 and 82 with methoxy, thiomethoxy and dimethylamino groups, D-A-D triads could be obtained (see Fig. 6). If 54 and 82 were determined as crystallizing in centrosymmetric arrangements, 81 crystallized in the P2<sub>1/C</sub> space group and showed an SHG response 80 times higher than the reference KDP.

In the previous studies of Fröhlich, substituents positioned on the 1,2,3-triazole ring were demonstrated to have no influence on

Table 4 Hyperpolarisability tensors in atomic units (a.u.) for the dyes 47 and 51–59								
Dyes	47	51	52	53	54	55	56	57
$\beta_{ m tot}$	0.37	0.41	0.51	1.72	2.39	2.69	4.44	2.48
Dyes				58				59
$\beta_{\text{tot}}$				2.52				3.19



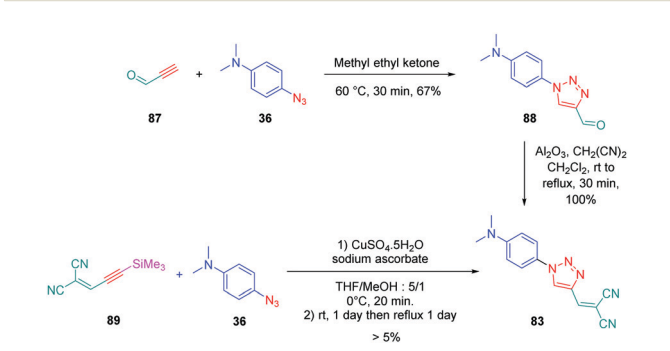
Chemical structures of 54, 81 and 82.

The four positional isomers of dicyanovinyl-triazole-dimethylaminobenzene compounds 83-86.

the SHG response, as quite similar responses were obtained with 1,2- and 1,4-regioisomers. This parameter was earlier studied by Diederich et al. and opposite conclusions were then established with 83-86 (see Fig. 7).51 For this study, if potentially seven constitutional isomers could be prepared differing in the position of the electron-donating and electron-accepting groups around the triazole group, only four of them 83-86 were obtained.

From a synthetic point of view, the design of these four dyes proved to be a challenge. As shown in Scheme 8, 83 could only be obtained using a two-step procedure, by first performing the click reaction with propynal 87 and 4-azido-N,N-dimethylaniline 36 and by subsequently realizing the Knoevenagel reaction of 88. Conversely, attempts of the click reaction with 4-azido-N,Ndimethylaniline 36 and 2-(3-(trimethylsilyl)prop-2-yn-1-ylidene)malononitrile 89 only furnished 83 in low reaction yields (>5%). The reaction of 2-(3-(trimethylsilyl)prop-2-yn-1-ylidene) malononitrile 89 and 4-azido-N,N-dimethylaniline 36 was more efficient to prepare the 1,2-regioisomer 90. In this last case, click chemistry was not the reaction used to prepare 90 but a thermal 1,3-dipolar cycloaddition. After 5 days of reflux, the intermediate silylated derivatives could be obtained in 18% yield and desilylation of 91 with methanol furnished 90 in 78% yield (see Scheme 9). If the reaction was low-yielding, the formation of 90 was highly selective, resulting from the bulkiness of the trimethylsilyl group.

Concerning 85 and 86, the two molecules were synthesized by alternative synthetic routes to click chemistry or the thermal



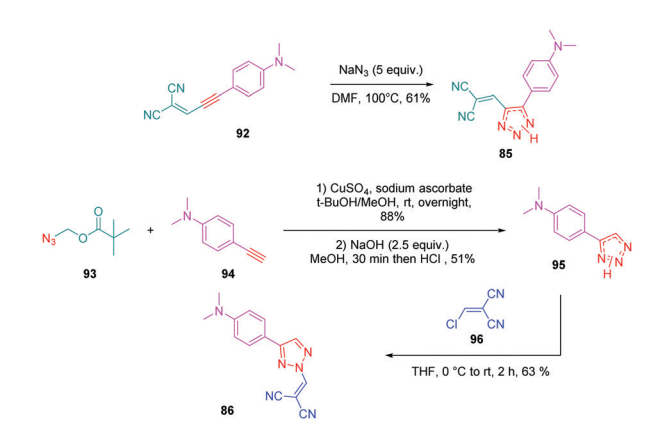
Scheme 8 Synthetic pathway of 83.

The two-step synthetic route to 90 Scheme 9

Huisgen reaction, these two procedures being unable to provide the two expected products. Thus, to prepare 85, a simple cycloaddition reaction of 2-(3-(4-(dimethylamino)phenyl)prop-2-vn-1-vlidene)malononitrile 92 with sodium azide upon heating at 100 °C formed 85 in 61% yield.

Conversely, 86 was obtained in more steps, the first one consisting of the click reaction between azidomethyl pivalate 93 and 4-ethynyl-N,N-dimethylaniline 94, furnishing after basic treatment 73 in 51% yield. By an addition/elimination reaction of N,N-dimethyl-4-(2H-1,2,3-triazol-4-yl)aniline 95 with (chloromethylidene) propanedinitrile 96 carried out at room temperature, 86 could be obtained in 63% yield (see Scheme 10).

To examine the effect of the 1,2,3-triazole ring on the electronic delocalization between the electron-donating dimethylaminophenyl group and the electron accepting dicyanomethylidene group, a comparison of the photophysical properties of 83-86 was established with those of 97<sup>52</sup> and 98<sup>53</sup> previously reported in the literature. Precisely, the nature of the spacer and the number of carbon atoms between the donor and the acceptor were determined in previous work of the same group as being determinants of the photophysical properties of the dyes. In this context, 97 and 98 were selected for the comparison due to the similarity in the length of their  $\pi$ -conjugated spacers (see Fig. 8 and Table 5).54



Scheme 10 Synthetic routes to 85 and 86

Chemical structures of 97 and 98

Optical properties of 83-86, 97 and 98

Dyes	$\lambda_{\mathrm{abs}} (\mathrm{nm})$	$\varepsilon \left( \mathrm{M^{-1}~cm^{-1}} \right)$	Ref.
83	400	8100	40
84	433	2500	40
85	423	11 300	40
86	453	7300	40
97	477	44 100	40
98	488	47 000	42

All spectra were recorded in CH2Cl2 at 298 K.

As the first finding, a clear reduction of the conjugation upon incorporation of the 1,2,3-triazole ring was determined for 83-86 relative to 97 and 98. A blue-shift as high as 88 nm was measured between the absorption maxima of 83 and 98. While examining the influence of the substitution pattern on the 1,2,3-triazole ring, the worst results were obtained upon substitution of nitrogen 1 of the triazole, clearly interrupting the conjugation in 83 and 84. Conversely, upon substitution of nitrogen 2 of the triazole with an electron accepting group, an absorption maximum at 453 nm was found for 86, shifted by 53 nm compared to 83 (see Table 5).

The well-established N.N-dimethylaminophenyl group was not the only electron donor to be used for the design of triazolebased push-pull dyes. Another electron-donating group of interest which is extensively used for the design of photoluminescent dyes was also employed, namely fluorene. Small molecules but also polymers<sup>55</sup> were prepared for their photoluminescence properties. Concerning small molecules, a series of four derivatives 99-101 varying in the substituent attached onto the electron accepting moiety was examined for their absorption and emission properties.<sup>56</sup> Using the standard conditions of click chemistry, the four compounds were obtained with reaction yields ranging from 72% for **99** to 79% for **100** and **101** by making a reaction between 103 with 34, 35 with 104 or 34 with 105 (see Scheme 11). Surprisingly, examination of the absorption properties revealed the absorption maximum for 102 to be blue-shifted compared to 99-101 (295 nm vs. 300 nm), whereas 102 is substituted by the most electron-withdrawing group (see Table 6).

This blue-shift is the opposite situation to what is classically observed upon introduction of a nitro group onto a push-pull chromophore. 57,58 The authors tentatively assigned this unexpected shift to a reduction of the conjugation length, the electron-accepting group extending from the triazole ring to the aromatic ring. This trend was confirmed by photoluminescence, 102 again exhibiting the most blue-shifted emission (334 nm vs. 353 nm for 99) (see Table 6). However, 102 was the most emissive compound of the series, its photoluminescence quantum yield peaking at 0.2%.

Scheme 11 Click chemistry reaction of four fluorene-triazole-pull molecules **99-102** 

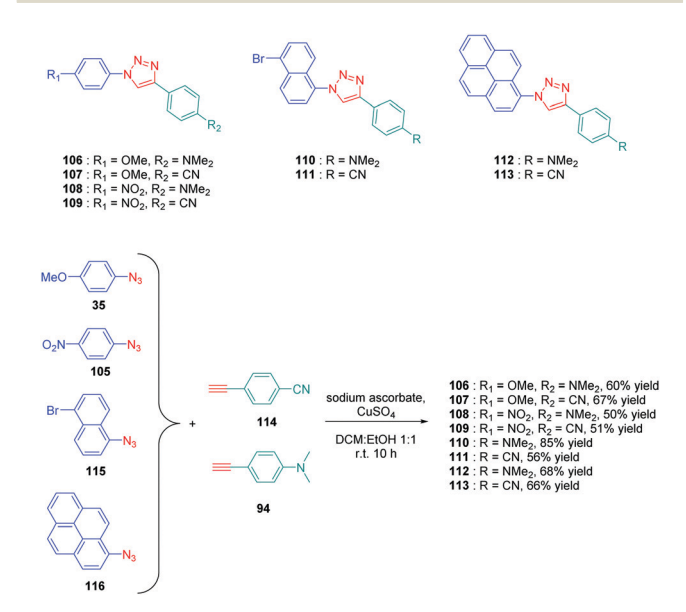
Table 6 Physical properties of the four fluorene derivatives 106-113 reported in ref. 56

Compounds	$\lambda_{abs}^{a}$ (nm)	$\lambda_{\mathrm{em}}^{}b}$ (nm)	$\Delta\lambda$ Stokes's (nm)	$\varepsilon (M^{-1} cm^{-1})$
99	300	353	53	8100
100	300	337	37	2500
101	300	339	39	11 300
102	295	334	39	7300

<sup>a</sup> Recorded in THF with  $c = 10 \mu M$  at room temperature. <sup>b</sup> Upon excitation at 297 nm.

The solvatochromism of 99-102 in eight solvents revealed the four dyes to be insensitive to the solvent polarity while examining their absorption characteristics. The opposite situation was found for their emission properties. If the emission of 102 was also insensitive to the solvent polarity, broadening of the absorption spectra was found for 100 and 101 whereas a clear red shift from 342 nm in toluene to 363 nm in acetonitrile was found for 99 upon increasing the solvent polarity. To support the strong shift observed for 99, the presence of excited state intramolecular charge transfer (ESICT) was proposed by the authors. This hypothesis was confirmed while using the Lippert-Mataga model. On the contrary, for 100 and 101, an admixture of locally excited (LE) emission and intramolecular charge transfer emission was proposed to explain the near insensitivity of the emission to the solvent polarity.

Determination of the origin of the photoluminescence properties was performed with another series of dyes 106-113 based on polyaromatic structures. 59 As the main interest of this study, the authors succeeded in converting non-fluorescent or low emissive compounds into highly emissive dyes by simply realizing a click reaction (see Scheme 12). By making a reaction between 4-ethynyl-N,N-dimethylaniline 94 and 4-ethynylbenzonitrile 114 with four different aryl azides 35, 105, 115 and 116, eight dyes 106-113 could be obtained with reaction yields ranging from 50 to 67%. As observed for the previous series of dyes, solvatochromism revealed



Scheme 12 Chemical structures of 106-113

the absorption maxima for all dyes to be not affected by the solvent

polarity contrarily to the photoluminescence maxima. Concerning photoluminescence, an increase of the PLQY with the solvent polarity was demonstrated, evidencing a highly polar excited state. The lack of influence of the solvent polarity on the absorption properties was also indicative of intramolecular charge transfer originating from the lowest-lying excited state. The shift of the emission maximum proved to be relatively important, as exemplified with 106, which showed a shift as high as 122 nm between hexane and methanol. Comparatively, 111 showed lower sensitivity, the shift being limited to 23 nm. Among the series of dyes, 112, which comprises a pyrene moiety, proved to be the most interesting compound from the point of view of its emission. If a structureless emission peak was found in apolar solvents (cyclohexane and hexane), dual emission could be detected in polar solvents, one of the two peaks being characteristic of the emission of pyrene. In fact, coexistence of ICT emission and LE emission was determined in the PL spectra. Examination of the solvatochromic behaviour by using the Lippert-Mataga model confirmed the previous conclusions. Notably, the different linear correlations revealed the ground state of these dyes to be moderately polar and the emissive state to be highly polar, corresponding to ICT emission. Due to the unique ability of 112 to exhibit dual emission in polar solvents, this compound constitutes thus an excellent candidate for polarity sensing.

Over the years, a wide range of 1,2,3-triazole-based fluorogenic dyes 117-123 have been developed, especially for biolabeling applications as exemplified with the series of compounds presented in Fig. 9.60-65 Indeed, in vivo bioimaging and theranostics are two active research fields requiring the rapid development of new structures. 66-72 In 2009, an extensive study was notably carried out on 102 dyes by making a reaction between 17 azides and 5 different xanthone or xanthene-based fluorophores.<sup>73</sup> However, conclusions were difficult to establish, no clear trend being detected. Concerning fluorenes, another series of dyes (124-131) was reported in 2013, incorporating diazines as electron acceptors.74

In this study, which required hard work for the synthesis with regards to the diversity of structures and the number

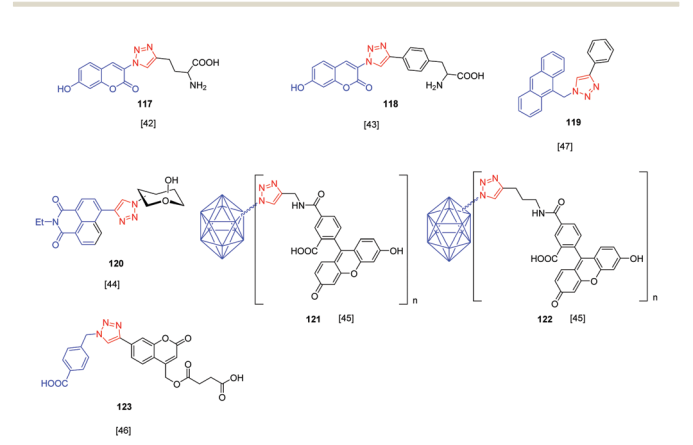


Fig. 9 Series of triazole-based dyes 117-123 used for biolabeling

Type I 
$$\begin{array}{c} F_{3} \\ F_{1} \\ F_{2} \\ F_{3} \\ F_{4} \\ F_{5} \\$$

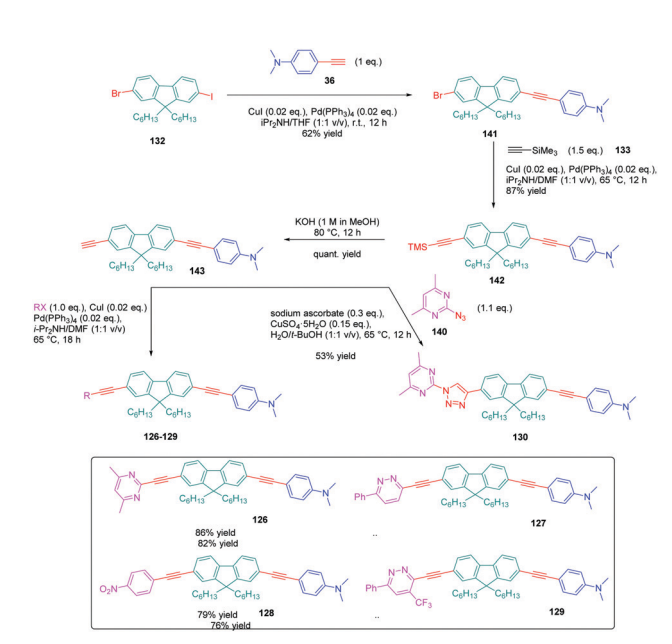
Fig. 10 Structures of the fluorene-based dyes 124-131 comprising a diazine (pyrimidine or pyridazine) as the electron accepting group.

of compounds, four series (I-IV) of D- $\pi$ -A diads were elaborated, comprising the fluorene unit as a spacer connecting the electronaccepting diazine to the electron-donating N,N-dimethylaminobenzene, and differing in the length of the  $\pi$ -conjugated spacer. The structures of the four series of dyes are presented in Fig. 10, comprising as diazine groups pyridazines<sup>75</sup> or pyrimidines.<sup>76</sup>

In turn, numerous combinations based on different linkages (two triazoles, one triazole and one ethynyl bridge, two ethynyl groups, and two  $\sigma$ -bonds) could be prepared. A reference compound with a nitro end-group was also prepared for comparison. To create asymmetric structures, 2-bromo-9,9-dihexyl-7-iodo-9H-fluorene 132 proved to be the key element for these different syntheses. Starting from this intermediate, a double Sonogashira cross-coupling reaction with trimethylsilyl-acetylene 133 and triisopropylacetylene 135 enabled the introduction of two ethynyl groups end-capped with protecting groups that could be cleaved selectively with different reaction conditions. Using this strategy, 131 could be obtained after 6 steps in moderate yield (see Scheme 13). A more versatile synthetic route was developed for 105-108 and 109 since a common intermediate could be prepared in three steps starting from 2-bromo-9,9-dihexyl-7-iodo-9H-fluorene 111. Finally, a Sonogashira coupling with the appropriate aryl halide could provide 105-108 with reaction yields ranging from 76 to 86% (see Scheme 14). Concerning 109, reaction of the common intermediate with azidopyrimidine following a CuAAC procedure could provide 109 in 53% yield.

A similar approach was developed for the synthesis of 144 and 145 based on a Suzuki cross-coupling reaction this time (see Scheme 15). Despite the presence of two different halogens on 2-bromo-9,9-dihexyl-7-iodo-9H-fluorene 132, the higher reactivity of the iodine atom over the bromine one was not totally respected, 20% of 4,4'-(9,9-dihexyl-9H-fluorene-2,7-diyl)bis(N,N-dimethylbenzenamine) 146 being obtained as a side-product of the reaction of 147 while using 4-dimethylaminobenzeneboronic

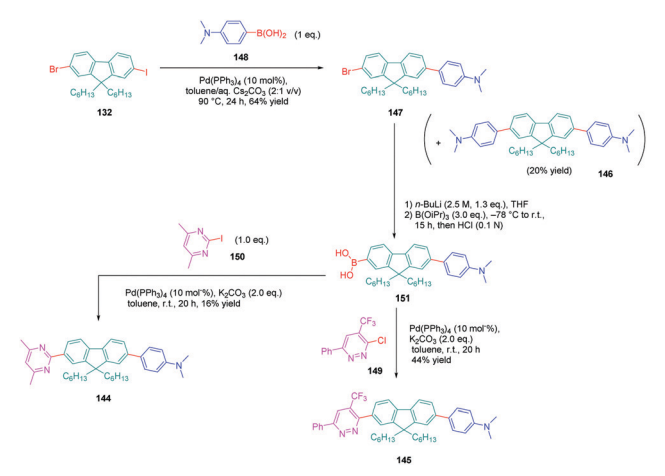
Scheme 13 Synthesis of the double triazole-bridged compound 131 starting from 132.



Scheme 14 Synthetic route to compounds 126-130

acid 148 (see Scheme 15). Surprisingly, a higher yield was obtained for the Suzuki cross coupling reaction of 3-chloro-6-phenyl-4-(trifluoromethyl)-pyridazine 149 (44% yield) than 2-iodo-4,6dimethylpyrimidine 150 (16% yield). Generally, higher reaction yields are obtained with iodo-derivatives than chloro-derivatives due to the higher polarization of the C-I bond. 77-85 In the present case, the higher reactivity of 3-chloro-6-phenyl-4-(trifluoromethyl)pyridazine 149 was assigned to the presence of the trifluoromethyl group, activating the C-Cl bond.

The UV-visible absorption and photoluminescence properties of the different dyes were examined in dichloromethane and a summary of the photophysical properties is provided in Table 7.



Successive Suzuki cross coupling reactions enabling the formation of the push-pull derivatives 144 and 145

Table 7 Photophysical properties of compounds 126-131, 144 and 145 reported in ref. 74

Dyes	$\lambda_{abs}$ (nm)	$\lambda_{\mathrm{em}}  (nm)$	Stokes shift (cm <sup>-1</sup> )	$\varepsilon \left( \mathbf{M}^{-1} \ \mathbf{cm}^{-1} \right)$
131	334	422	6243	82 000
130	362	450	5402	71 500
128	391	474	4478	51 900
129	392	500	5510	74 700
127	377	539	7972	58 100
126	372	515	7464	52094
145	358	423	4292	39 300
144	360	483	7074	58 800

Considering that all dyes possess the same electron donating group but differ in the electron accepting group and the nature of the conjugated spacer, a comparison could be established.

First, all dyes exhibited an absorption maximum located in the UV-visible range. The maximum absorption was determined at 334 nm for 131 and 392 nm for 129, which possess the most red-shifted absorption of the series. For a similar electron-donating moiety, a dramatic decrease of the PLQY was determined for 145. Indeed, compared to 144 for which a PLQY of 0.69 was measured, this value decreased to 0.01 for 145, this compound being almost not emissive.

This result was assigned to the presence of the CF<sub>3</sub>-group inducing a torsion of the molecule and breaking the  $\pi$ -conjugation. The comparison between 126, 127 and 129 and the reference compound 128 revealed an appreciable red-shift of the emission maxima upon replacing the nitrobenzene group of 128 by diazine groups. The most red-shifted emission was found for 127, peaking at 539 nm. Introduction of the electron-withdrawing trifluoromethyl-pyridazine group in 129 did not significantly modify the absorption maximum compared to 128. Finally, using 126, 130, 131 and 144 exhibiting the same electron donating and accepting groups, the influence of the linkage could be determined. Thus, while replacing a single bond by an ethynyl spacer and triazole rings, a significant enhancement of the molar extinction coefficient could be determined, peaking at 82 000 M<sup>-1</sup> cm<sup>-1</sup> for 131. Conversely, a blue-shift of the absorption maximum was

**Table 8** Two photon absorption cross-sections  $\delta_{\text{TPA}}$  and wavelength of the maximum TPA cross-section reported in ref. 74

Dyes	$\lambda_{\text{TPA}}^{a}$ (nm)	$\delta_{\text{TPA}}^{\ \ b} \left(10^{-50} \text{ cm}^4 \text{ s photon}^{-1}\right)$
131	700	39
130	760	148
128	750	114
129	740	367
127	780	269
126	760	82
144	700	263
145	740	123

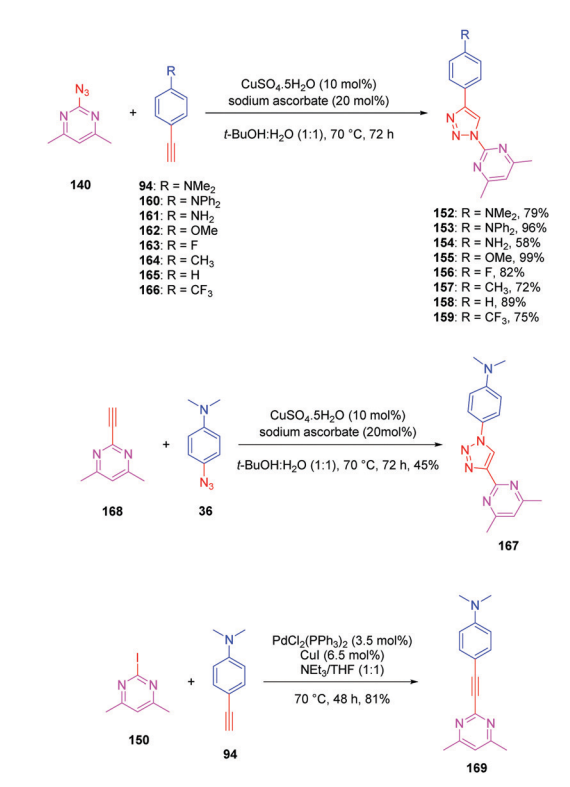
<sup>&</sup>lt;sup>a</sup> Wavelength of the maximum TPA cross-section. <sup>b</sup> TPA cross-section.

found for 131 compared to 144 (334 nm vs. 360 nm respectively), evidencing a clear interruption of the conjugation when a 1,2,3triazole ring is introduced as the spacer. Finally, two photon absorption (TPA) measurements were realized on these molecules and the results are summarized in Table 8. By using a femtosecond laser pulse, the solutions could be excited in the 690-940 nm region. All triazole-based dyes displayed a maximum wavelength for the TPA absorption in the near infrared region. While comparing 126, 130 and 131, the benefits of the presence of one triazole ring were clearly evidenced, the TPA absorption being shifted from 740 to 760 nm. Conversely and as observed for photoluminescence, the presence of two triazole rings in 131 was detrimental for the photophysical properties, a blue-shift as high as 60 nm being detected for the TPA maximum wavelength between 144 and 131.

The pyrimidine moiety has been at the basis of numerous push-pull dyes, this group constituting a relatively good electron acceptor. Notably, a series of eight push-triazole-pull dyes 152-159 differing in the end-groups was synthesized using the click reaction. This series was achieved by click chemistry between the azidopyrimidine 140 and the different alkynes 94 and 160-166 in a mixture of water/tert-butanol, in the presence of copper sulfate and sodium ascorbate, producing the eight dyes 152-159 with reaction yields ranging from 58 to 99% (see Scheme 16). Here again, two structural analogues of 152 were prepared, the first one (167) resulting from a click reaction between 4,6 dimethyl-2-ethynylpyrimidine 168 and 4-azido-N,N-dimethylaniline 36. Synthesis of this compound 167 was previously reported in the literature (see Scheme 16).86,87

The second one (169) was obtained by a Sonogashira cross coupling reaction of 2-iodo-4,6-dimethylpyrimidine 150 with 4-ethynylaniline 94, providing the compound in 81% yield (see Scheme 16).

As anticipated, all dyes exhibited absorption centered in the UV region, ranging from 244 nm for 156 to 222 nm for 153. Conversely, part of the molecules could emit in the visible range, from 476 nm for 153 and 154 to 486 nm for 152. A major impact of the substitution pattern was demonstrated. Thus, alkylation of the amine group of 154 resulted in a red-shift of both the absorption and the emission properties of 152 and 153 due to an improved electron-donating ability. Conversely, the methoxy group is a less efficient electron donor than a dimethylamino or a diphenylamino group, which was confirmed by the



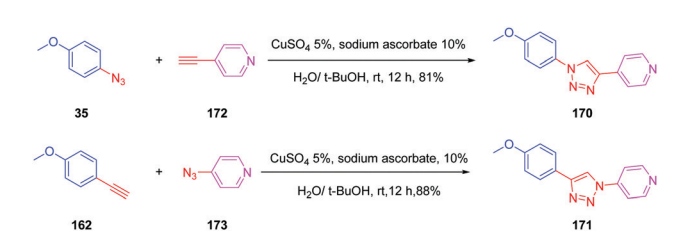
Scheme 16 Synthesis of the triazole-based series 152-159, 167 and 169 and the corresponding reaction yields.

blue-shift of both the absorption and the emission peaks of 154 (see Table 9). While comparing 152 and 167, inversion of the triazole ring in 167 resulted in a blue-shift of the absorption and the emission maxima, together with a decrease of the PLQY.

**Table 9** Two photon absorption cross-sections  $\delta_{\mathsf{TPA}}$  and wavelength of the maximum TPA cross-section reported in ref. 85

Dyes	$\lambda_{abs} \ (nm)$	$\epsilon \left( M^{-1} \ cm^{-1} \right)$	$\lambda_{em} \ (nm)$	Stokes shift (cm <sup>-1</sup> )	$\Phi_{ ext{F}}{}^a$
152	289	24 386	486	14 026	0.47
153	333	21 427	476	9022	0.45
154	267	25 698	476	16 445	0.30
155	254	46 211	389	13 663	0.01
156	244	18 069	345	11 998	< 0.01
157	250	18 943	364	12 527	< 0.01
158	246	25 697		_	
159	254	20 753		_	
167	250	13 893	434	16 958	0.33
169	357	42 161	447	5640	0.04

All spectra were recorded in  $CH_2Cl_2$  at 25 °C. a Quantum yield ( $\pm 10\%$ ) of fluorescence determined by using harmane in 0.1 M H<sub>2</sub>SO<sub>4</sub> as a standard ( $\Phi_F = 0.83$ ).



Scheme 17 Synthesis of pyridyloxazole-type fluorophores 170 and 171

On replacement of the triazole ring in 152 and 167 by an ethynyl group, a drastic red-shift of the absorption maximum occurred (357 nm vs. 250 nm for 167). On the contrary, the small Stokes shift and the low PLQY of 167 confirmed the conclusions previously established from a similar comparison. To get a deeper insight into the optical properties of the different dyes, DFT calculations were carried out. For most of the compounds a

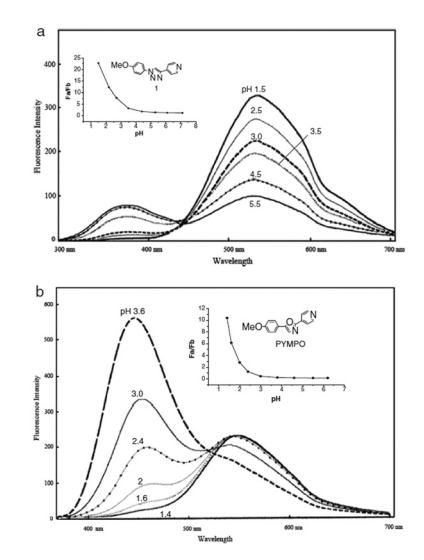


Fig. 11 Fluorescence emission spectra of PYMPO (b) and its triazolebased analogue 170 (a). Reproduced with permission from ref. 88. Copyright 2007, The Chemical Society of Japan (CSJ).

Scheme 18 One pot process for synthesis of quinoxalines 174-187.

fully planar structure was found except for 167, which presented a dihedral angle of 35° between the phenyl ring and the triazole ring.

This deviation supports the blue-shift observed both in absorption and emission for 167 relative to 152. Theoretical calculations also revealed the absorption spectrum of 169 to be dominated by two main transitions, assigned to the HOMO  $\rightarrow$ LUMO and the HOMO-1  $\rightarrow$  LUMO transitions. Considering that for all triazole-based dyes a unique transition corresponding to the HOMO → LUMO transition could be theoretically determined, comparison between 169 and 152 or 167 is relatively difficult. Besides, the higher PLQY of 152 compared to 169 is indicative of better electron transfer when a triazole ring is used. Parallel to this, DFT calculations also showed the

**Table 10** Two photon absorption cross-sections  $\delta_{\text{TPA}}$  and wavelength of the maximum TPA cross-section reported in ref. 91

	$R_1$	$R_2$	Product	Yield	λ <sub>max</sub> , abs <sup>a</sup> [nm]	λ <sub>max</sub> , em <sup>b</sup> [nm]
174	N N	C Sur	Ph N=N N	82	262	541
175	N.	C Port	Ph N=N N	77	292	548
176	China China	C Sari	Ph N=N N=N N-N Ph	56	393	n.d.
177	S	C Prof.	Ph N=N N N	72	259	n.d.
178	N. N	C Profe	Ph N=N	42	293	n.d.
179	N Ja	C) soft	Ph N=N	62	384	613
180	S	C Park	Ph N=N	66	n.d.	440
181	S Br	C Sari	Ph N=N N=N N N	70	n.d.	n.d.

n.d.: not determined. <sup>a</sup> Recorded in  $CH_2Cl_2$ ,  $C = 10^{-5}$  M at T = 293 K. Recorded in CH2Cl2.

electron density of 152 to be more separated than in 169. Indeed, if the LUMO level of 169 extends over the phenyl ring of the donor, conversely, for 152, the LUMO level is strictly confined on the electron accepting group. In this context, a higher electronic redistribution occurs upon excitation of 152 compared to 167. The influence of the orientation of the phenyl ring on the optical properties was not limited to diazine-based electron acceptors. Pyridine was also selected as a candidate for carrying out a similar study.88 The synthetic route is reported in Scheme 17 and the two dyes 170 and 171 could be obtained with reaction yields close to 90%.

Specifically, 170 and 171 were prepared for their structural analogy to PYMPO, which is a pH probe characterized by strong emission but which is difficult to prepare.<sup>89,90</sup> Considering that pyridine is highly sensitive to the pH of the reaction medium and can potentially be protonated under acidic conditions, and that the 1,2,3-triazole ring can be easily formed starting from

easily accessible intermediates, 170 and 171 were thus considered as candidates of choice to act as a pH probe to examine biological samples in vivo. Examination of the PL spectra at pH below 7 revealed the fluorescence intensity of 170 to decrease while increasing the pH. No modification of the emission maxima was also detected while varying the pH. Comparison of the PL spectra of 170 and 171 revealed a major difference in the number of peaks. Thus, if two peaks could be detected in the PL spectra of 170, a unique peak could be found for 171, irrespective of the pH (see Fig. 11). Finally, comparison of 170 with PYMPO revealed a 25-fold enhancement of the pH-sensitivity of 170 for pH ranging from 1.5 to 7.

Luminescent molecules can also be obtained using a complex procedure as exemplified in the following series of fluorophores. 91 Fourteen 3-triazolylquinoxaline derivatives 174-188 were notably prepared using a glyoxylation-alkynylation-cyclocondensation-Cu-catalyzed alkyne-azide cycloaddition (GACC-CuAAC) sequence

**Table 11** Two photon absorption cross-sections  $\delta_{\text{TPA}}$  and wavelength of the maximum TPA cross-section reported in ref. 91

	$R_1$	$R_2$	Product	Yield	$\lambda_{\max}$ , abs <sup>a</sup> [nm]	$\lambda_{\text{max}}$ , em <sup>b</sup> [nm]
174	N N	int.	Ph N=N	82	262 292 393	541
182	N N		Ph N=N N	73	n.d.	n.d.
183	N.	CI	N=N N=N	48	265 396	541
184	N N	- Set	N=N N=N N=N	79	n.d.	n.d.
185		F	F-N=N N=N N	58	265 396	547
186	N N	o pri	N=N N=N	46	263 290 392	541
187	N N	J. p. s.	N=N N N	69	264 292 391	540

n.d.: not determined. <sup>a</sup> Recorded in  $CH_2Cl_2$ ,  $C = 10^{-5}$  M at T = 293 K. <sup>b</sup> Recorded in  $CH_2Cl_2$ .

requiring five components to proceed. In this one pot reaction, coupling glyoxylation of rich  $\pi$ -electron heterocycles, Castro alkynylation of acyl chlorides by alkynes, and cyclocondensation of diketones with diphenylamine followed by a click reaction of various azide derivatives 194-204 with alkynes 189-193 furnished 174-188 with reaction yields ranging from 42% for 178 to 82% for 174 (see Scheme 18). Two series of molecules can be distinguished. As shown in Table 10, the first series (174-181) differs from the second one by the nature of the electron donating  $\pi$ -heterocycles. Conversely, the second series (182-187) varies only in the substituents on the triazole ring, the other substituents remaining the same (see Table 11). If change of the electron donating  $\pi$ -heterocycles could impact the emission wavelength, modification of the pendant group introduced by means of the azide derivatives did not significantly change the photophysical properties of the second series of compounds (see Tables 10 and 11).

In fact, by improving the electron-donating ability of the heterocycle, a bathochromic shift was observed from 2-thienyl (180) to 1-methylpyrrolyl (175), 1-indolyl (174) and finally dimethylaminobenzene (179) groups. Using this strategy, a red-shift of the absorption maximum from 368 nm for 180 to 393 nm for 179 was observed. For all dyes, relatively low PLQYs were determined, and this counter-performance was assigned to an internal torsion in the ground and the excited states resulting from the presence of the triazole ring. DFT studies confirmed the lack of influence of the triazolyl substituents on the intramolecular charge transfer, since the HOMO is localized on the rich-electron heterocycle and the LUMO on the quinoxaline core. Moreover, optimization of the geometries of all dyes confirmed the rotation of the triazolyl ring, impacting the conjugation of this substituent with the rest of the molecule. This absence of an effect of the appended triazole ring on the photophysical properties could constitute an advantage for future applications of quinoxalozine compounds in materials or biological applications.

## 3. Conclusions

The discovery of click chemistry at the beginning of the 21st century has clearly reinvented the way to produce molecules. The effect of triazole on the photophysical properties has been clearly evidenced over the years. If the presence of the 1,2,3triazole ring has clearly demonstrated a negative impact on the  $\pi$ -conjugation when used as a spacer in push-pull dyes, benefits of this group were also demonstrated by providing a higher Stokes shift and higher PLQYs to molecules comprising this group. Besides, by its easiness to be handled and the different studies reporting the preparation of numerous derivatives, the advantages of click chemistry to rapidly develop a wide range of derivatives have been clearly demonstrated. Considering the versatility of click chemistry, the reduction of  $\pi$ -conjugation in push–pull dyes compared to alkene, alkyne and other  $\pi$ -conjugated spacers will certainly be solved in the future. Concerning the future applications in which click-chemistry-based dyes could be involved, photopolymerization, which is a rapidly expanding research field,

is one of those. Notably, photopolymerists are searching new dyes with optical properties that could be finely tuned allowing to efficiently initiate and control a polymerization process. The same exigence exists for non-linear optical applications with the design of dyes with carefully controlled absorption properties. The versatility of click chemistry will certainly allow during the next decade the design of efficient photoinitiators or NLO dyes.

### Conflicts of interest

There are no conflicts to declare.

## **Acknowledgements**

This research was funded by Aix-Marseille University and the Centre National de la Recherche Scientifique. The Direction Générale de l'Armement (DGA) is acknowledged for its financial support through the PhD grant of Damien Brunel.

#### References

- 1 C. W. Tornøe, C. Christensen and M. Meldal, J. Org. Chem., 2002, 67, 3057-3064.
- 2 V. V. Rostovtsev, L. G. Green, V. V. Fokin and K. B. Sharpless, Angew. Chem., Int. Ed., 2002, 41, 2596-2599.
- 3 R. Huisgen, G. Szeimies and L. Möbius, Chem. Ber., 1967, 100, 2494-2507.
- 4 X. Jiang, X. Hao, L. Jing, G. Wu, D. Kang, X. Liu and P. Zhan, Expert Opin. Drug Discovery, 2019, 14, 779-789.
- 5 P. Thirumurugan, D. Matosiuk and K. Jozwiak, Chem. Rev., 2013, 113, 4905-4979.
- 6 J.-P. Meyer, P. Adumeau, J. S. Lewis and B. M. Zeglis, Bioconjugate Chem., 2016, 27, 2791-2807.
- 7 A. Marrocchi, A. Facchetti, D. Lanari, S. Santoro and L. Vaccaro, Chem. Sci., 2016, 7, 6298-6308.
- 8 D. Döhler, P. Michael and W. H. Binder, Acc. Chem. Res., 2017, 50, 2610-2620.
- 9 K. Kacprzak, I. Skiera, M. Piasecka and Z. Paryzek, Chem. Rev., 2016, 116, 5689-5743.
- 10 V. K. Tiwari, B. B. Mishra, K. B. Mishra, N. Mishra, A. S. Singh and X. Chen, Chem. Rev., 2016, 116, 3086-3240.
- 11 A. Saeed, F. A. Larik and P. A. Channar, Res. Chem. Intermed., 2016, 42, 6805-6813.
- 12 N. G. Aher, V. S. Pore, N. N. Mishra, A. Kumar, P. K. Shukla, A. Sharma and M. K. Bhat, Bioorg. Med. Chem. Lett., 2009, 19, 759-763.
- 13 M. Meldal and C. W. Tornøe, Chem. Rev., 2008, 108, 2952-3015.
- 14 J. E. Moses and A. D. Moorhouse, Chem. Soc. Rev., 2007, 36, 1249-1262.
- 15 M. Juricek, P. H. J. Kouwer and A. E. Rowan, Chem. Commun., 2011, 47, 8740-8749.
- 16 P. Xiao, W. Hong, Y. Li, F. Dumur, B. Graff, J.-P. Fouassier, D. Gigmes and J. Lalevée, Polym. Chem., 2014, 5, 2293-2300.
- 17 P. Xiao, F. Dumur, D. Thirion, S. Fagour, A. Vacher, X. Sallenave, B. Graff, J.-P. Fouassier, D. Gigmes and J. Lalevée, Macromolecules, 2013, 46, 6786-6793.

- 18 P. Xiao, F. Dumur, T. T. Bui, X. Sallenave, F. Goubard, B. Graff, F. Morlet-Savary, J.-P. Fouassier, D. Gigmes and J. Lalevée, ACS Macro Lett., 2013, 2, 736–740.
- 19 P. Xiao, F. Dumur, B. Graff, D. Gigmes, J.-P. Fouassier and J. Lalevée, *Macromolecules*, 2013, 46, 7661–7667.
- 20 A. Al Mousawi, F. Dumur, J. Toufaily, T. Hamieh, B. Graff, D. Gigmes, J.-P. Fouassier and J. Lalevée, *Macromolecules*, 2017, 50, 2747–2758.
- 21 J. Zhang, N. Zivic, F. Dumur, P. Xiao, B. Graff, D. Gigmes, J.-P. Fouassier and J. Lalevée, *J. Polym. Sci., Part A: Polym. Chem.*, 2015, 53, 445–451.
- 22 P. Xiao, M. Frigoli, F. Dumur, B. Graff, D. Gigmes, J.-P. Fouassier and J. Lalevée, *Macromolecules*, 2014, 47, 106–112.
- 23 M.-A. Tehfe, F. Dumur, B. Graff, F. Morlet-Savary, D. Gigmes, J.-P. Fouassier and J. Lalevée, *Polym. Chem.*, 2013, 4, 3866–3875.
- 24 M. Parent, O. Mongin, K. Kamada, C. Katan and M. Blanchard-Desce, *Chem. Commun.*, 2005, 2029–2031.
- 25 P. D. Zoon, I. H. M. van Stokkum, M. Parent, O. Mongin, M. Blanchard-Desce and A. M. Brouwer, *Phys. Chem. Chem. Phys.*, 2010, 12, 2706–2715.
- 26 L. Porrès, O. Mongin, C. Katan, M. Charlot, T. Pons, J. Mertz and M. Blanchard-Desce, *Org. Lett.*, 2004, **6**, 47–50.
- 27 M. G. Silly, L. Porrès, O. Mongin, P. A. Chollet and M. Blanchard-Desce, *Chem. Phys. Lett.*, 2003, **379**, 74–80.
- 28 H. Qin, S. Wenger, M. Xu, F. Gao, X. Jing, P. Wang, S. M. Zakeeruddin and M. Grätzel, *J. Am. Chem. Soc.*, 2008, 130, 9202–9203.
- 29 H. Li, K. Fu, A. Hagfeldt, M. Grätzel, S. G. Mhaisalkar and A. C. Grimsdale, *Angew. Chem.*, *Int. Ed.*, 2014, **53**, 4085–4088.
- 30 G. Zhang, H. Bala, Y. Cheng, D. Shi, X. Lv, Q. Yu and P. Wang, *Chem. Commun.*, 2009, 2198–2200.
- 31 H. Im, S. Kim, C. Park, S.-H. Jang, C.-J. Kim, K. Kim, N.-G. Park and C. Kim, *Chem. Commun.*, 2010, **46**, 1335–1337.
- 32 W. Zeng, Y. Cao, Y. Bai, Y. Wang, Y. Shi, M. Zhang, F. Wang,C. Pan and P. Wang, *Chem. Mater.*, 2010, 22, 1915–1925.
- 33 P. Blanchard, C. Malacrida, C. Cabanetos, J. Roncali and S. Ludwigs, *Polym. Int.*, 2019, **68**, 589–606.
- 34 R. Rybakiewicz, M. Zagorska and A. Pron, *Chem. Pap.*, 2017, 71, 243–268.
- 35 A. Cravino, S. Roquet, O. Alévêque, P. Leriche, P. Frère and J. Roncali, *Chem. Mater.*, 2006, **18**, 2584–2590.
- 36 M. Bourass, A. T. Benjelloun, M. Benzakour, M. Mcharfi, F. Jhilal, M. Hamidiband and M. Bouachrine, *New J. Chem.*, 2017, 41, 13336–13346.
- 37 T. Duan, K. Fan, Y. Fu, C. Zhong, X. Chen, T. Peng and J. Qin, *Dyes Pigm.*, 2012, **94**, 28–33.
- 38 S. Wen, J. Pei, Y. Zhou, P. Li, L. Xue, Y. Li, B. Xu and W. Tian, *Macromolecules*, 2009, **42**, 4977–4984.
- 39 K. Sharma, V. Sharma and S. S. Sharma, *Nanoscale Res. Lett.*, 2018, **13**, 381.
- 40 F. Lenzmann, J. Krueger, S. Burnside, K. Brooks, M. Grätzel, D. Gal, S. Rühle and D. Cahen, *J. Phys. Chem. B*, 2001, **105**, 6347–6352.
- 41 P. Kautny, D. Bader, B. Stöger, G. A. Reider, J. Fröhlich and
   D. Lumpi, *Chem. Eur. J.*, 2016, 22, 18887–18898.

- 42 C. Katan, P. Savel, B. M. Wong, T. Roisnel, V. Dorcet, J. L. Fillaut and D. Jacquemin, *Phys. Chem. Chem. Phys.*, 2014, **16**, 9064–9073.
- 43 N. Mataga, Y. Kaifu and M. Koizumi, *Bull. Chem. Soc. Jpn.*, 1956, **29**, 465-470.
- 44 J. L. Oudar and D. S. Chemla, J. Chem. Phys., 1977, 66, 2664–2668.
- 45 S. Gronowitz and T. Frejd, *Chem. Heterocycl. Compd.*, 1978, 14, 353–367.
- 46 B. Iddon, Heterocycles, 1983, 20, 1127-1171.
- 47 T. L. Gilchrist, Adv. Heterocycl. Chem., 1987, 41, 41-74.
- 48 D. Lumpi, E. Horkel, B. Stoeger, C. Hametner, F. Kubel, G. A. Reider and J. Froehlich, *Proc. SPIE*, 2011, 8306, 830615/1.
- 49 D. Lumpi, F. Glöcklhofer, B. Holzer, B. Stöger, C. Hametner, G. A. Reider and J. Fröhlich, *Cryst. Growth Des.*, 2014, 14, 1018–1031.
- 50 D. Lumpi, J. Steindl, S. Steiner, V. Carl, P. Kautny, M. Schön, F. Glöcklhofer, B. Holzer, B. Stöger, E. Horkel, C. Hametner, G. Reider, M. D. Mihovilovic and J. Fröhlich, *Tetrahedron*, 2017, 73, 472–480.
- 51 P. D. Jarowski, Y.-L. Wu, W. B. Schweizer and F. Diederich, *Org. Lett.*, 2008, **10**, 3347–3350.
- 52 K. Staub, G. A. Levina, S. Barlow, T. C. Kowalczyk, L. S. Lackritz, M. Barzoukas, A. Fort and S. R. Marder, *J. Mater. Chem.*, 2003, **13**, 825–833.
- 53 T. Michinobu, J. C. May, J. H. Lim, C. Boudon, J. P. Gisselbrecht, P. Seiler, M. Gross, I. Biaggio and F. Diederich, *Chem. Commun.*, 2005, 737–739.
- 54 B. B. Frank, P. R. Laporta, B. Breiten, M. C. Kuzyk, P. D. Jarowski, W. B. Schweizer, P. Seiler, I. Biaggio, C. Boudon, J.-P. Gisselbrecht and F. Diederich, *Eur. J. Org. Chem.*, 2011, 4307–4317.
- 55 D. J. V. C. van Steenis, O. R. P. David, G. F. P. van Strijdonck, J. H. van Maarseveen and J. N. H. Reek, *Chem. Commun.*, 2005, 4333–4335.
- 56 Y. Zhu, S. Guang, X. Su, H. Xu and D. Xu, *Dyes Pigm.*, 2013, 97, 175–183.
- 57 G. Kremser, O. T. Hofmann and S. Sax, *Monatsh. Chem.*, 2008, **139**, 223–231.
- 58 Y. L. Liu, J. K. Feng and A. M. Ren, *J. Phys. Chem. A*, 2008, **112**, 3157–3164.
- 59 S. S. Bag and R. Kundu, J. Org. Chem., 2011, 76, 3348-3356.
- 60 K. E. Beatty, J. C. Liu, F. Xie, D. C. Dieterich, E. M. Schuman, Q. Wang and D. A. Tirrell, *Angew. Chem., Int. Ed.*, 2006, 45, 7364–7367.
- 61 K. E. Beatty, F. Xie, Q. Wang and D. A. Tirrell, *J. Am. Chem. Soc.*, 2005, **127**, 14150–14151.
- 62 M. Sawa, T.-L. Hsu, T. Itoh, M. Sugiyama, S. R. Hanson, P. K. Vogt and C.-H. Wong, *Proc. Natl. Acad. Sci. U. S. A.*, 2006, 103, 12371–12376.
- 63 Q. Wang, T. R. Chan, R. Hilgraf, V. V. Fokin, K. B. Sharpless and M. G. Finn, *J. Am. Chem. Soc.*, 2003, **125**, 3192–3193.
- 64 Z. Zhou and C. J. Fahrni, J. Am. Chem. Soc., 2004, 126, 8862-8863.
- 65 F. Xie, K. Sivakumar, Q. Zeng, M. A. Bruckman, B. Hodges and Q. Wang, *Tetrahedron*, 2008, **64**, 2906–2914.
- 66 D. Li, S. Wang, Z. Lei, C. Sun, A. M. El-Toni, M. S. Alhoshan, Y. Fan and F. Zhang, *Anal. Chem.*, 2019, 91, 4771–4779.

Perspective

- 67 F. Ding, C. Li, Y. Xu, J. Li, H. Li, G. Yang and Y. Sun, Adv. Healthcare Mater., 2018, 7, 1800973.
- 68 R. Zhang, Y. Xu, Y. Zhang, H. S. Kim, A. Sharma, J. Gao, G. Yang, J. S. Kim and Y. Sun, Chem. Sci., 2019, 10, 8348-8353.
- 69 L. Tua, Y. Xu, Q. Ouyang, X. Li and Y. Sun, Chin. Chem. Lett., 2019, 30, 1731-1737.
- 70 F. Ding, Y. Fan, Y. Sun and F. Zhang, Adv. Healthcare Mater., 2019, 8, 1900260.
- 71 F. Ding, Z. Chen, W. Y. Kim, A. Sharma, C. Li, Q. Ouyang, H. Zhu, G. Yang, Y. Sun and J. S. Kim, Chem. Sci., 2019, 10, 7023-7028.
- 72 Y. Xu, M. Tian, H. Zhang, Y. Xiao, X. Hong and Y. Sun, Chin. Chem. Lett., 2018, 29, 1093-1097.
- 73 J. Li, M. Hu and S. Q. Yao, Org. Lett., 2009, 11, 3008-3011.
- 74 C. Denneval, O. Moldovan, C. Baudequin, S. Achelle, P. Baldeck, N. Plé, M. Darabantu and Y. Ramondenc, Eur. J. Org. Chem., 2013, 5591-5602.
- 75 S. Achelle, N. Plé and A. Turck, RSC Adv., 2011, 1, 364–388.
- 76 S. Achelle and N. Plé, Org. Synth., 2012, 9, 163-187.
- 77 A. F. Littke and G. C. Fu, Angew. Chem., Int. Ed., 2002, 41, 4176-4211.
- 78 B. U. W. Maes, P. Tapolcsányi, C. Meyers and P. Mátyus, Curr. Org. Chem., 2006, 10, 377-417.
- 79 S. Nara, J. Martinez, C. G. Wermuth and I. Parrot, Synlett, 2006, 3185-3204.

- 80 A. Turck, N. Plé, L. Mojovic and G. Queguiner, Bull. Soc. Chim. Fr., 1993, 130, 488-492.
- 81 S. Achelle, N. Plé, A. Turck, J. P. Bouillon and C. Portella, J. Heterocycl. Chem., 2006, 43, 1243-1249.
- 82 S. Achelle, Y. Ramondenc, F. Marsais and N. Plé, Eur. J. Org. Chem., 2008, 3129-3140.
- 83 S. Tumkevicius, J. Donkova, I. Baskirova and A. Voitechovicius, J. Heterocycl. Chem., 2009, 46, 960-964.
- 84 S. Asano, S. Kamioka and Y. Isobe, Tetrahedron, 2012, 68, 272-279.
- 85 A. S. Cornec, C. Baudequin, C. Fiol-Petit, N. Plé, G. Dupas and Y. Ramondenc, Eur. J. Org. Chem., 2013, 1908-1915.
- 86 K. D. Grimes, A. Gupte and C. C. Aldrich, Synthesis, 2010, 1441-1448.
- 87 T. Sakamoto, M. Shiraiwa, Y. Kondo and H. Yamanaka, Synthesis, 1983, 312-314.
- 88 J. Shi, L. Liu, J. He, X. Meng and Q. Guo, Chem. Lett., 2007, 36, 1142-1143.
- 89 S. Charier, O. Ruel, J.-B. Baudin, D. Alcor, J.-F. Allemand, A. Meglio and J. Jullien, Angew. Chem., Int. Ed., 2004, 43, 4785.
- 90 S. Charier, O. Ruel, J.-B. Baudin, D. Alcor, J.-F. Allemand, A. Meglio, L. Jullien and B. Valeur, Chem. - Eur. J., 2006, 12, 1097-1113.
- 91 F. K. Merkt, K. Pieper, M. Klopotowski, C. Janiak and T. J. J. Müller, Chem. - Eur. J., 2019, 25, 9447-9455.